STM JOURNALS

Trends in
Electrical Engineering

https://journals.stmjournals.com/tee

ISSN: 2249-4774 (Online)
ISSN: 2321-4260 (Print)
Volume 15, Issue 2, 2025
May–August
DOI (Journal): 10.37591/TEE

Research TEE

Electromagnetic Transients in Compensated Overhead Lines with Multiple Tower Spans

Mohamed Mostafa Saied[1,*]

Abstract

This paper addresses the analysis of the electromagnetic transients developed in an important class of non-uniform high-voltage power lines. It deals particularly with compensated long overhead high-voltage transmission lines composed of several tower spans, which are connected in cascade. The derived mathematical model leads to a system composed of simultaneous partial differential and algebraic equations, which can be solved numerically in terms of parametric functions using the software Mathematica's statement (ParametricNDSolve). The resulting current and voltage distributions along the line will be functions of the location x, the Laplace operators, as well as of the levels of eventually existing series capacitive and parallel inductive compensation. A code based on the Hosono algorithm can then be used for the numerical Laplace inversion of these expressions in order to get the corresponding results in the time-domain. The results of several representative case studies are presented and discussed in order to assess the impact of the different network parameters on the voltage and current distributions as well as the stresses in the compensating elements. It is believed that this study will be helpful to the high voltage and protection engineers, in addition to the power engineering students and trainees.

Keywords: Electromagnetic, transients, simulation, high-voltage lines, non-uniform, compensation, *Mathematica*, towers, span, partial differential equations, parametric functions, numerical Laplace inversion, Hosono algorithm, parameter study

INTRODUCTION

Analyses, mitigation, and protection against transient stresses developed in high-voltage power networks have attracted the interest of researchers, especially in recent years [1–13]. A large percentage of the resulting investigations have focused on issues related to overhead transmission lines and/or underground cables [6–13]. Most numerical solution approaches can be broadly classified as time-domain and Laplace domain based techniques [4–8]. Nonlinear situations, such as corona discharges and magnetic saturation, require time-domain solutions [6, 7, 9–13]. In some cases, special consideration is devoted to the location dependence of the circuit parameters of the transmission lines [13]. Uniform lines can be approximated as independent, which is a mainstream or traditional situation. Practical and more realistic non-uniform lines appear in several interesting cases, such as river crossings and high-voltage towers. To the best of our knowledge, no detailed information is available on the combined effect of the simultaneous presence of non-uniform overhead lines (e.g., in cases involving cascade-connected multi-tower spans) and the eventual presence of compensating elements.

The concept of series compensation is based on the addition of series capacitors to fully or partially eliminate the series inductive reactance, which is

***Author for Correspondence**
Mohamed Mostafa Saied
E-mail: mmsaied002@gmail.com

[1]Professor (Emeritus- Kuwait University), Independent Researcher, IEEE Life Senior Member, Giza, Cairo, Egypt

Received Date: April 07, 2025
Accepted Date: April 11, 2025
Published Date: August 29, 2025

Citation: Mohamed Mostafa Saied. Electromagnetic Transients in Compensated Overhead Lines with Multiple Tower Spans. Trends in Electrical Engineering. 2025; 15(2): 1–9p.

expressed by the per-unit compensation parameter k_{ser}. Shunt compensation, on the other hand, is achieved through the connection of parallel compensating coils to (at least partially) eliminate (of k_{sh} per unit of the line's shunt charging current. This study contributes to this area of research.

Strictly speaking, the proper selection of the sizes and locations of the compensating capacitors and coils is usually the result of rigorous optimization procedures with technical and/or economic objective functions and constraints. Without the loss of generality, this study considers the case in which the series compensating capacitor, *C*, and the shunt compensating coil, *L*, are placed at the line sending end (i.e., *x*=0) and its receiving end (*x=length*), respectively, as shown in Figure 1.

For the given values of the compensation parameters k_{ser} and k_{sh}, the following two equations can be derived to identify the required compensating elements *C* and *L:*

$$C = 1/[\omega 2.(total\ line\ inductance).k_{ser}]$$

and

$$L = 1/[\omega 2.(total\ line\ capacitance).k_{sh}]$$

Where, ω is the rated angular frequency (i.e., 314 rad./s for 50 Hz).

THE METHOD OF ANALYSIS

This paper addresses the combined effect of the conductors' sag, the eventual presence of line series capacitive and/or shunt inductive compensation, and the waveform of the initiating stimuli on the electromagnetic transients in high-voltage lines. The analysis starts with the derivation of a set of simultaneous algebraic and partial differential equations governing the voltage and current distributions in terms of both Laplace operator *s* and location *x*. They should consider the relevant initial and boundary conditions. An efficient *Mathematica* code is suggested for the numerical solution.

To the best of the authors' knowledge, no detailed information is currently available in the literature on the combined presence of non-uniformity of lines, such as those including cascaded multi-tower spans, as well as the presence of compensating elements. This study contributes to this area of research.

Because both the line inductance *l* and capacitance *c* per-unit length of the non-uniform line are assumed to be functions of the location *x*, the surge impedance zo will correspondingly change with *x*, as schematically shown in Figure 1.

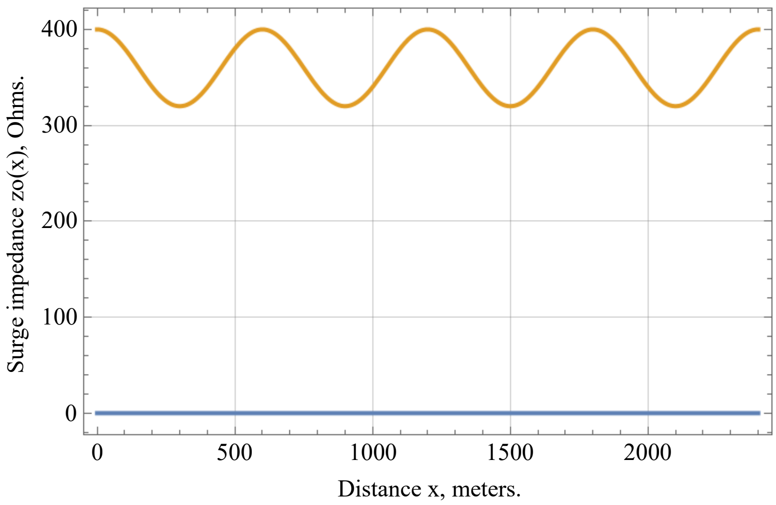

Figure 1. The line's surge impedance *zo(x)* as a function of the location *x*.

The plot depicts zo(x) over the distance between x=0 and x=2400 m of the sample overhead line. The plot covers ten span lengths of four tower spans, 600 m each. If the number of span lengths considered is N=4, the following expression can be derived:

$$\text{zo}(x) = 360 + 40\cos(2.pi.x/span) \text{ Ohms} \tag{1}$$

This is plotted in Figure 1 over four span lengths, that is, the coordinate x ranges between zero and 2400 m. zo(x) varied between the maximum and minimum values of 400 and 320 Ω, respectively.

From the well-known relations among the speed of light, surge impedance zo, and line parameters per meter l and c, the following relations can be derived:

$$c(x) = \frac{1}{\text{speed.zo}(x)} \tag{2}$$

$$l(x) = \frac{\text{zo}(x)}{\text{speed}} \tag{3}$$

The investigation starts with Equation (1), expressing the location dependence of the line's surge impedance $zo(x)$ as a function of the location x, measured from the line's source terminal for an overhead line of span length *span* between two consecutive towers.

This is illustrated by the plot in Figure 1 describing a 2.4-km overhead line having six equidistant towers and a span length of 600 m. The surge impedance sag was 20%. The surge impedance $zo(x)$ exhibits its highest value (400 Ω) at the tower locations and its lowest value (320 Ω) at the midpoint between two neighboring towers.

The line's transient response is governed by the following simultaneous partial differential equations:

$$\frac{\partial v}{\partial x} = -l(x)\frac{\partial i}{\partial t} - i.r, \tag{4}$$

And

$$\frac{\partial i}{\partial x} = -c(x)\frac{\partial v}{\partial t} \tag{5}$$

Where, r denotes the series resistance per-unit length of the line, which is assumed to be 0.1 mΩ/m. Their solution should consider the boundary conditions expressed in terms of the assumed source voltage and the line's receiving end termination impedance expressed in the s-Domain. For instance, this impedance can assume values of zero, infinity, $s.L$, $1/(sC)$ for the short-circuit, open circuit, inductive termination by inductance L, or capacitive termination by capacitance C, respectively.

The above system of equations can be solved for the s-domain expressions of the voltage and current using ParametricNDSolve of the software *Mathematica* (for example, Version 13.3) [14]. The time response can then be obtained through the use of the previously mentioned Hosono's algorithm for the numerical Laplace inversion [15].

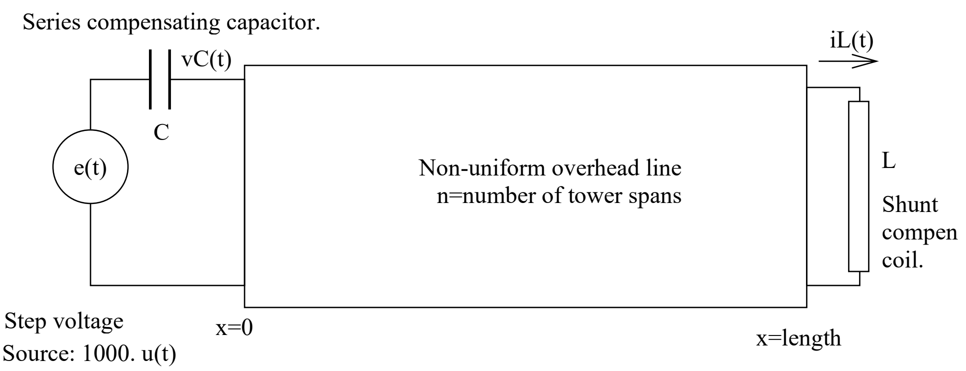

Figure 2. The considered sample power network.

SAMPLE RESULTS

As a representative example, this section presents the transient response of a fully compensated 2400-m-long non-uniform line composed of four tower spans, 600 m each, overhead line. The source voltage was assumed to be a 1000 V step voltage. Snapshots of the instantaneous voltage and current distributions at time point t-=t_{end} are depicted in the two plots, Figures 3(a) and (b), respectively. As expected, at the source (x=0), the voltage was 1000 V as expected. The initial value of is observed to be exactly 2.5 A. This agrees with the assumed source voltage (1000 V) and the value of the surge impedance of the line (400 Ω).

The computed transient response of the voltage developed across the series compensating capacitor, the current flowing through the shunt compensating coil, and its transient voltage are illustrated in Figure 3(c)–(e). The capacitor voltage transient assumed an average value of 1000 V and includes a superimposed oscillating high-frequency (250 kHz) transient component with an amplitude close to 5.5 V.

The current through the shunt compensating coil is plotted in Figure 3(e) using a more convenient logarithmic current axis. It varies between zero and several kiloamperes. The plot shows the distinct series and parallel resonance conditions at time points t=2, 2.6, 4, 5, etc. The voltage assumed a zero value at t=4 µs, coinciding with the maximum current value as well as its first peak at approximately t=0.4 µs. As observed in the two plots in Figure 3(e).

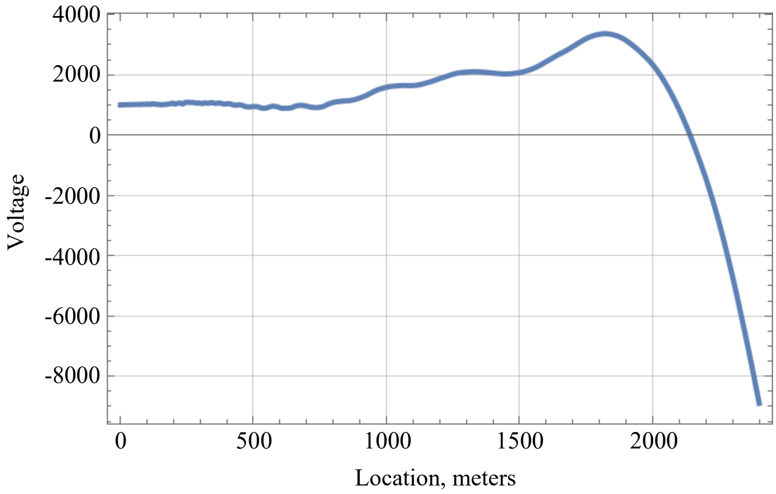

Figure 3. (a) Snapshot of the instantaneous voltage along the line at t=t_{end}.

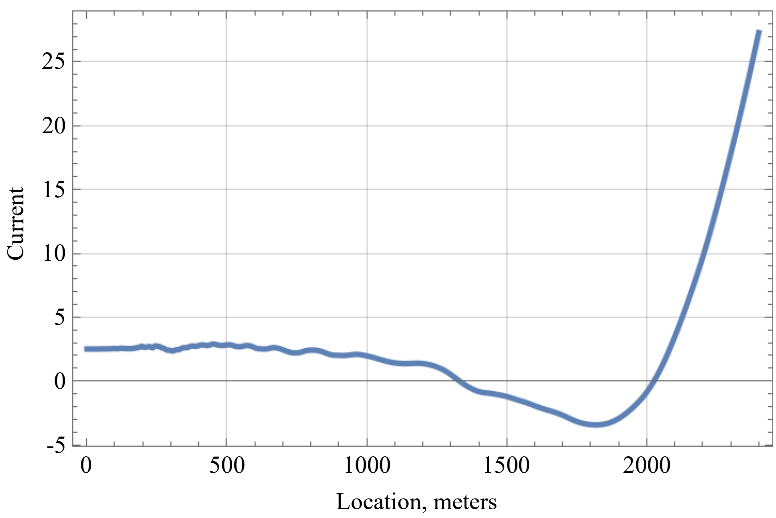

Figure 3. (b) Snapshot of the instantaneous current along the line at t=t_{end}.

Trends in Electrical Engineering
Volume 15, Issue 2
ISSN: 2249-4774 (Online), ISSN: 2321-4260 (Print)

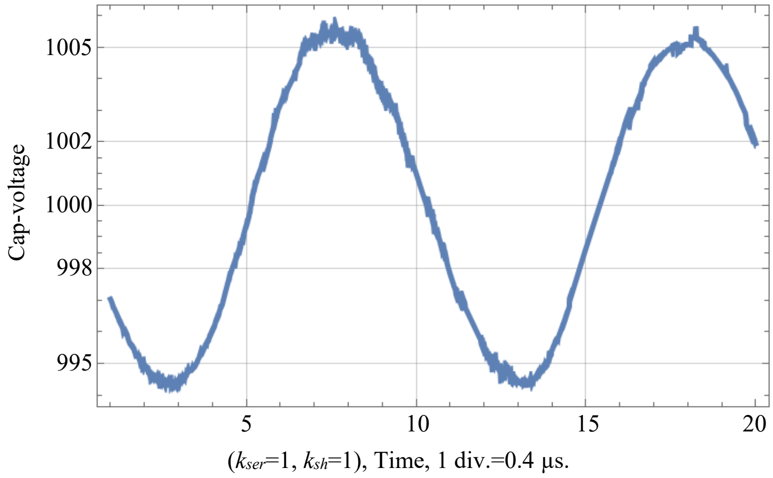

Figure 3. (c) The transient voltage across the series compensating capacitors.

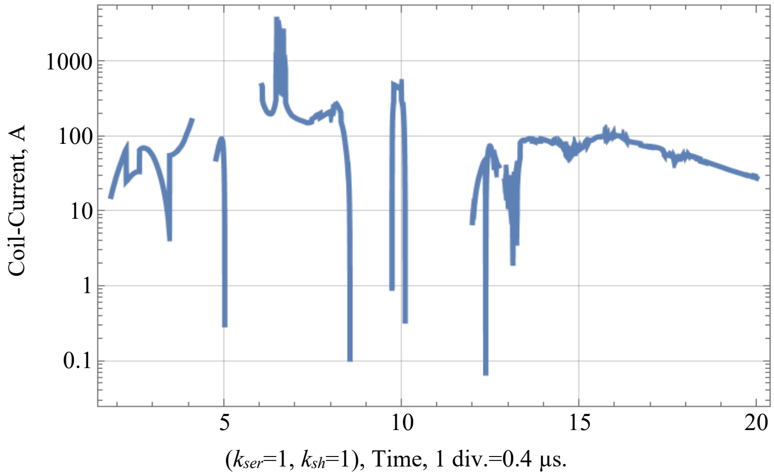

Figure 3. (d) The transient current flowing through the shunt compensating coil (in log scale).

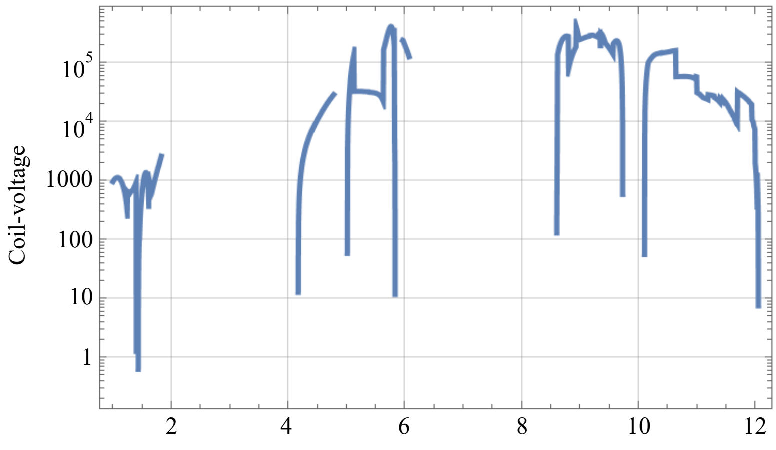

Figure 3. (e) The transient voltage developed across the shunt compensating coil (in log scale).

The plots illustrated in Figure 4 provide the results pertinent to a fully compensated overhead line having 20-tower spans, 600 meters each. Voltage profile at t=t_{end} = 40 µs is shown in Figure 4(a). It assumes an expected value of 1 kV at the line's source terminal and exhibits several minima and maxima at different locations along the line. The corresponding current profile is shown in plot in Figure 4(b) with the expected value of 2.74 A at the source.

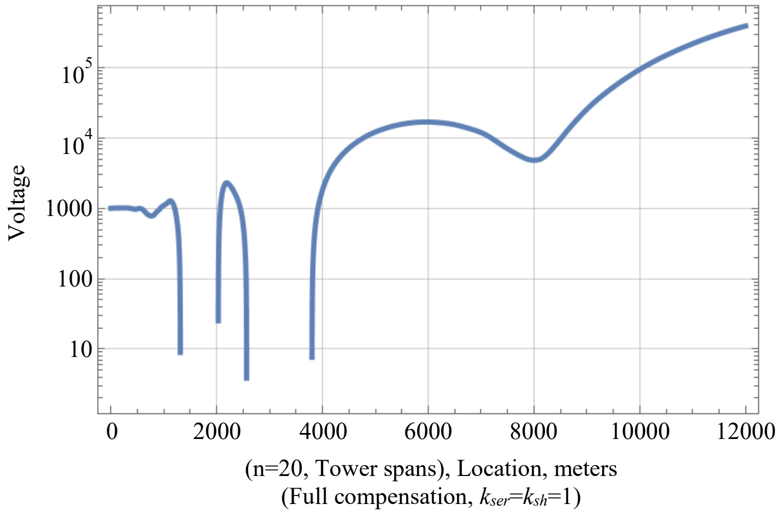

Figure 4. (a) Snapshot of the instantaneous voltage along the line at t=t_{end}.

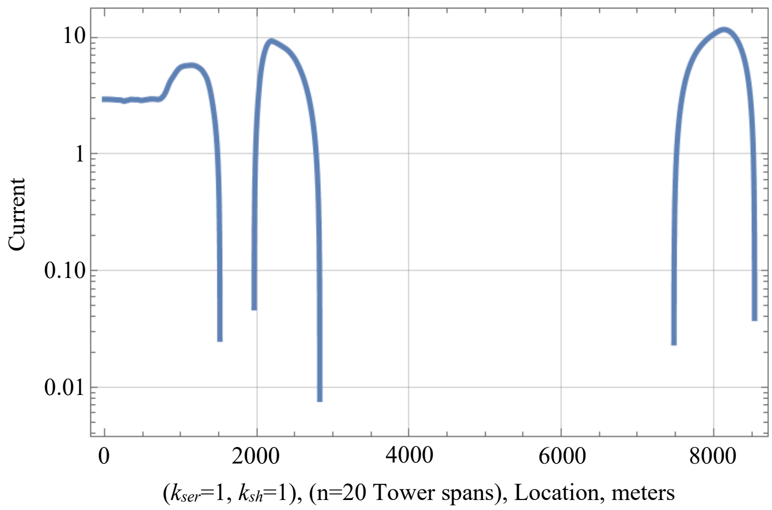

Figure 4. (b) Snapshot of the instantaneous current along the line at t=t_{end}.

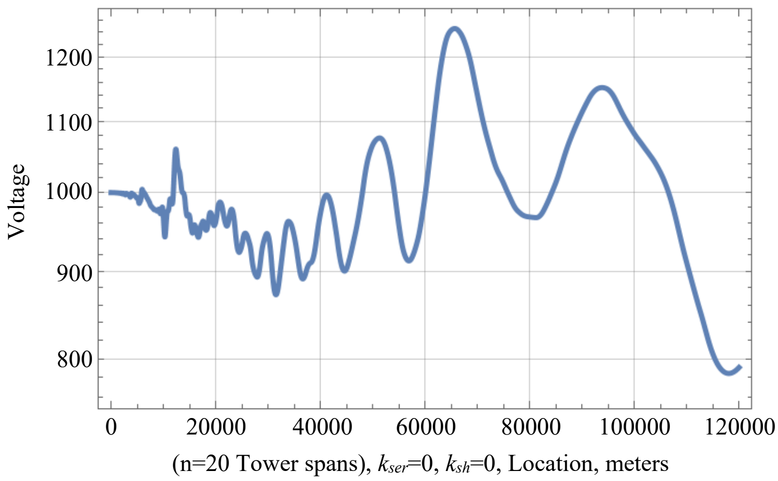

Figure 4. (c) Snapshot of the instantaneous voltage along the line at t=t_{end}, with zero compensation.

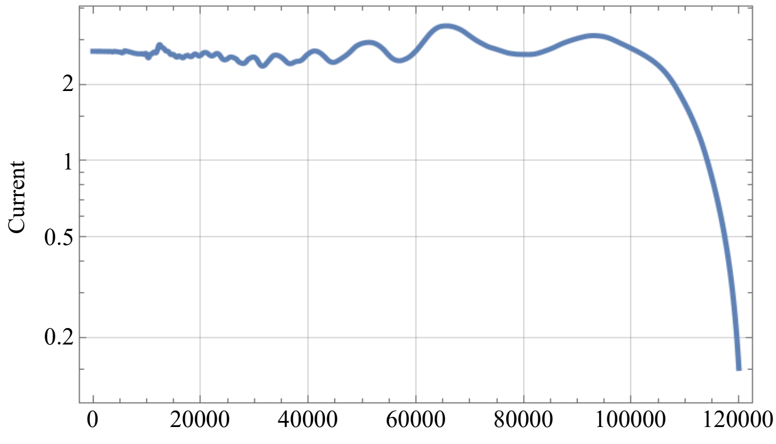

Figure 4. (d) Snapshot of the instantaneous current along the line at t=t_{end}.

With full compensation, and according to Figure 4(b), the current can momentarily reach values close to 10A at the two locations x= 2400 m and 8200 m. It has very small magnitudes at points close to 1500, 2000, 2800, 7500, and 8400 m.

The distributions of the transient voltage and current in the uncompensated case are shown in Figure 4(c) and (d), respectively. The voltage varies within the range of 760 V near the shunt compensating coil and 1230 V near the midpoint of the line. The current profile prevailing in the case of k_{ser}=0 and k_{sh}=0 is illustrated in plot in Figure 4(d). It exhibits two expected values of 2.74 A and zero A at the line's source and coil terminals, respectively.

VALIDATION

This section discusses the validation of the proposed method of analysis and the developed *Mathematica* computer code. A special case study with the following data was considered.

- Per-unit series compensation: k_{ser}=0.
- Per-unit shunt compensation: k_{sh}=0.
- A uniform overhead line with the constant surge impedance zo=365 Ohm.
- Number of tower spans: n = 5.
- Equal tower spans: 600 meters each.
- t_{end} (the solution's time range) = 100 µs.
- The magnitude of the source step voltage =1000 V.
- One division on the time scale corresponds to 5 µs.

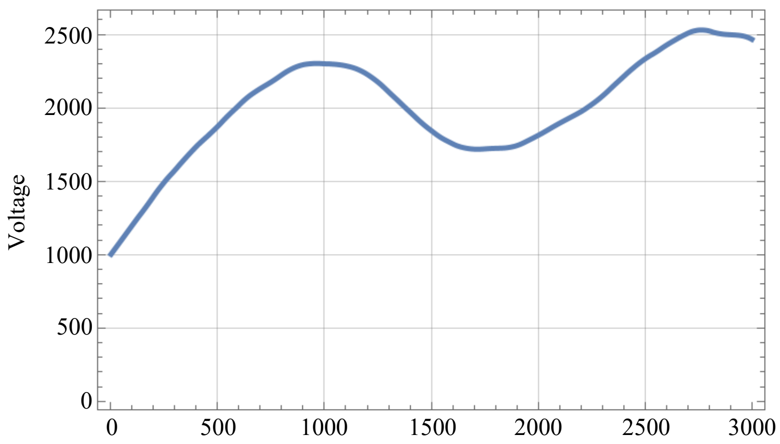

Figure 5. (a) Snapshot of the voltage distribution.

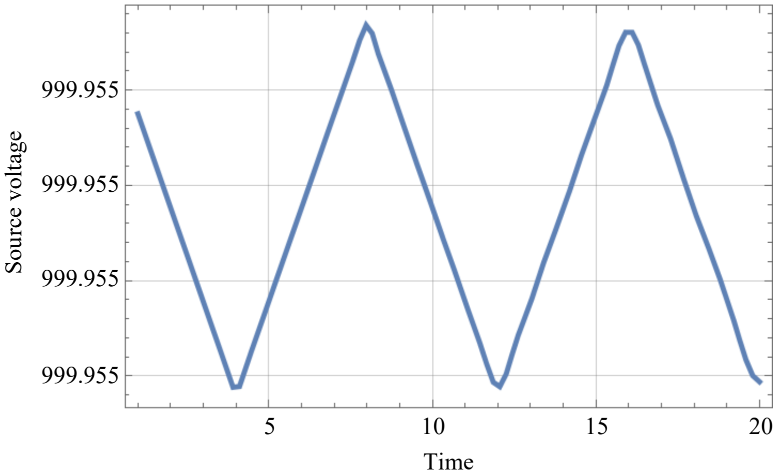

Figure 5. (b) The voltage at the line's sending end *(x*=0*)*.

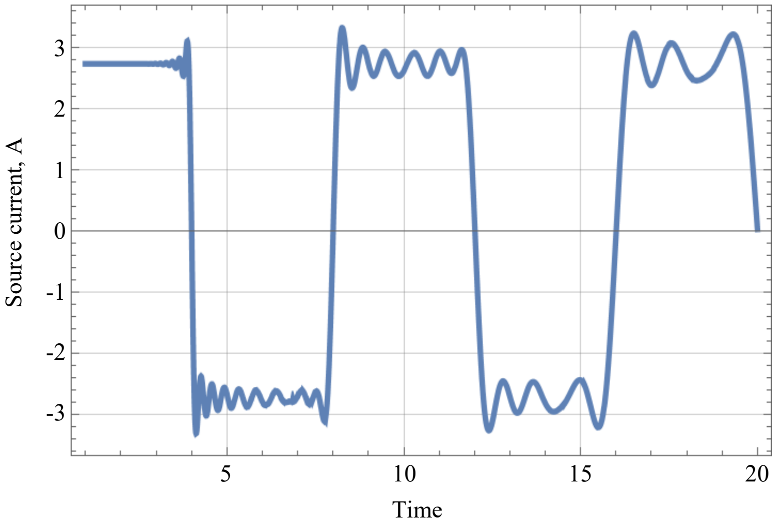

Figure 5. (c) The current at the line's sending end *(x*=0*)*. Time scale: one division =5 μs.

The computed voltage profile is shown in Figure 5(a). The voltage values were 1000 V and 2500 V at the two locations *x*=0 and *x*=3000 m, respectively. The computed voltage magnitude at the source terminal (*x*=0) is shown in Figure 5(b). Its magnitude is practically constant and equal to the initially assumed source voltage of 1000 V, as expected. The transient source current is shown in Figure 5(c). It starts with the expected value of 2.74A at *t*=0 and remains constant until *t*= 20 μs, which is exactly double the wave travel from the source to the shunt coil.

CONCLUSIONS

This study addresses the characteristics of long high-voltage overhead transmission lines composed of multiple equidistant tower spans. Any number of towers could be addressed. The presented model can consider the time waveforms of the sources initiating the transients, the lines' data and circuit parameters, as well as their loading conditions. This paper presents detailed analysis and a computer program for investigating electromagnetic transients and the existing corona current. The derived system of governing simultaneous differential and algebraic equations is solved numerically using a *Mathematica c*omputer code in terms of parametric equations and functions in the Laplace domain. The program yields *s*-domain expressions for the voltage and current distributions. The corresponding time-domain results were obtained through numerical Laplace inversion using the Hosono algorithm. This paper discussed the results of several case studies involving step- and ramp-form voltage sources,

ISSN: 2249-4774 (Online), ISSN: 2321-4260 (Print)

e(t), as well as pure resistive, pure capacitive, open circuit, and short-circuit line terminations. Among other facts, the results indicate that shunt corona currents, if any, can assume values of several amperes per kilometer.

REFERENCES

1. El Dein AZE, Gouda OE, Lehtonen M, Darwish MMF. Mitigation of the electric and magnetic fields of 500-kV overhead transmission lines. IEEE Access. 2022;10:33900-8. doi:10.1109/ACCESS.2022.3161932.
2. Bewley LV. Traveling Waves on Transmission Systems. New York: Dover; 1963.
3. Greenwood A, Selzer A. Electrical transients in power systems. IEEE Trans Syst Man Cybern. 1973;SMC–3:301–2. doi:10.1109/TSMC.1973.4309230
4. Dommel HW. Bonneville Power Administration. Electromagnetic Transients Program Reference Manual: (EMTP) Theory Book. Portland, OR: Bonneville Power Administration; 1986.
5. Van der Sluis L. Transients in Power Systems. New York: John Wiley & Sons; 2001. doi:10.1002/0470846186.
6. Begamudre RD. Extra High-Voltage AC Transmission Engineering. New Delhi: New Age International; 2006.
7. Ovick NL. Travelling waves on transmission lines, including corona effects [dissertation]. Pittsburgh: University of Pittsburgh; 1982.
8. Scharlemann E. An EMTP Theory Book Correction. LLNL-TR-450052. Livermore, CA: Lawrence Livermore National Laboratory; 2010.
9. Saied M, Safar Y, Salama M. Line transients with corona. J Univ Kuwait Sci. 1987;14:77–95.
10. Saied MM, Safar YA. Electromagnetic transients on compensated lines under corona. Electr Mach Power Syst. 1989;16:441–62. doi:10.1080/07313568908909401.
11. Tarditi AG, Besnoff JS, Duckworth R, Li FR, Li Z, Liu Y, Mcconnell BW, Olsen RG, Poole BR, Piesciorovsky EC, et al. High voltage modeling and testing of transformer, line interface devices, and bulk system components under electromagnetic pulse, geomagnetic disturbance, and other abnormal transients [Internet]. Oak Ridge (TN): Oak Ridge National Laboratory (US); 2019. doi: https://doi.org/10.2172/1515663.
12. Saied MM. Corona modeling for the transient analysis, steady state and corona loss performance of transmission lines. Electr Power Qual Util J. 2013;16(2):11–20.
13. Sellschopp FS, Arjona LM. An automated system for frequency response analysis with application to an undergraduate laboratory of electrical machines. IEEE Trans Educ. 2004;47:57–64. doi:10.1109/TE.2003.817621.
14. Wolfram S. Differential equation solving with DSOLVE. Champaign, IL: Wolfram Research; 2008.
15. Hosono T. Numerical inversion of Laplace transform and some applications to wave optics. Radio Sci. 1981;16:1015–9. doi:10.1029/RS016i006p01015.
16. Lingaiah V. Exploring transmission lines overhead light. South Asian J Mark Manag Res. 2022 Jan;12(1, Suppl):97–107.

